DOI: 10.1002/cssc.201100430

Flexible and Platinum-Free Dye-Sensitized Solar Cells with Conducting-Polymer-Coated Graphene Counter Electrodes

Kun Seok Lee,[a] Youngbin Lee,[b] Jun Young Lee,[a] Jong-Hyun Ahn,*[b] and Jong Hyeok Park*[a]

Dye-sensitized solar cells (DSSCs) have emerged as a high-efficiency, low-cost alternative to solid-state silicon solar cells.[1–3] Typically, DSSCs are composed of a mesoporous titania nanocrystal electrode on a transparent conductive oxide (TCO) substrate with ruthenium-based sensitizers on the titania nanocrystals, platinum on the TCO substrate as a counter electrode, and iodine/iodide electrolyte between the two TCO substrates.[4] The high costs of these materials is an obstacle and prevents the commercialization of DSSCs. In particular platinum, which has a high conductivity, high catalytic activity, and is stable, is one of the most expensive components in DSSCs.[5] To reduce costs, the development of alternative materials for use in DSSCs is needed.

Another important issue for commercialization is finding a method to produce flexible DSSCs, because this would enable the fabrication of light-weight, thin, and low-cost DSSCs through roll-to-roll mass production.[6,7] Several methods for fabricating titania nanoparticle films (for use as photoanode) or platinum (for use as counter electrode) on a TCO-coated plastic film have been devised. Poly(ethylene terephthalate) coated with indium-doped tin oxide (ITO–PET) is one of the best flexible TCO substrates. However, ITO–plastic substrates are well-known to easily lose their conductivity during bending tests, resulting in low stabilities compared to electrodes that use glass substrates. Hence, the development of next-generation flexible DSSCs is focused on replacing platinum and inorganic material-based TCOs simultaneously.

The first to be considered as alternatives to platinum were carbon-based materials, such as activated carbon, carbon nanotubes, graphite, carbon black, and graphene, which have been used as catalysts for DSSCs.[8–13] In a recent study, a carbon-based counter electrode achieved a power conversion efficiency of ca. 9%, which is comparable to that of platinum-based DSSCs.[13a] Another approach to platinum-free counter electrodes used several conducting polymers and obtained maximum conversion efficiencies of ca. 7.8% from poly(3,4-alkylenedioxythiophene),[14] 7.1% from microporous polyaniline,[15a] 7.07% from a nanographite/polyaniline composite,[15b] and 7.93% from poly(3,4-alkylenedioxythiophene) nanoporous layers prepared by electro-oxidative polymerization.[16] However, there have been few reports on platinum- and TCO-free counter electrodes achieving cell efficiencies comparable to Pt/TCO counter electrodes. Typical platinum-free counter electrode materials have been prepared on TCO substrates and showed efficiencies of over 9%.[13] Because the TCO is also expensive, the next development for cost-effective counter electrodes should be the simultaneous omission of platinum and the TCO.[17]

Our group has reported DSSC counter electrodes with conducting polymers, replacing both platinum and the TCO substrate.[17] Because the conducting polymer should, in addition to inducing an electrochemical reaction, also transport charges, highly conductive poly(3,4-ethylenedioxythiophene) (PEDOT) films are essential. When only PEDOT films without TCO were used as counter electrode in the fabrication of DSSCs, a power conversion efficiency of 5.08% was obtained. In the *J–V* curves, the J_{sc} and V_{oc} values were comparable values to those of Pt/FTO based DSSCs, but the main obstacle were the low FF values, due to the low surface conductivity of PEDOT. Given that the polymer does not have a conductivity comparable to that of commercialized TCOs, there is still scope to improve the cell efficiency without resorting to the use of a TCO as substrate.

Owing to its high conductivity, graphene has recently attracted attention as an alternative to TCOs for various electronic applications, such as displays, solar cells, and sensors.[18–21] Several developments in its large-area synthesis and the transfer of high-quality graphene films onto a target substrate have created new pathways for the application of graphene to flexible devices.[22] Herein, we report the cell performances of DSSCs with graphene, overcoated with a PEDOT film, on flexible target substrates. These were used as counter electrode without using additional TCO. The high conductivity of the graphene layer provides a further decrease of the surface resistance. Furthermore, the graphene/PEDOT counter electrodes fabricated on plastic substrates show very good mechanical flexibility.

Figure 1 is an illustration detailing the fabrication steps of the graphene/PEDOT counter electrode on a PET substrate. First large-area, high-quality graphene films were grown on a rectangular piece of copper foil (thickness 25 μm) by using procedures described elsewhere.[23,24] In brief, an annealing process with hydrogen gas cleans a surface of the copper catalyst material and expands grain size of the copper to synthesize high-quality graphene. After hydrocarbon atoms are ad-

[a] *K. S. Lee, Prof. J. Y. Lee, Prof. J. H. Park*
School of Chemical Engineering and
SKKU Advanced Institute of Nanotechnology
Sungkyunkwan University
Suwon 440-746 (Korea)
Fax: (+82) 31-290-7272
E-mail: lutts@skku.edu

[b] *Y. Lee, Prof. J.-H. Ahn*
School of Advanced Materials Science and Engineering and
SKKU Advanced Institute of Nanotechnology
Sungkyunkwan University
Suwon 440-746 (Korea)
Fax: (+82) 31-290-7400
E-mail: ahnj@skku.edu

Supporting Information for this article is available on the WWW under http://dx.doi.org/10.1002/cssc.201100430.

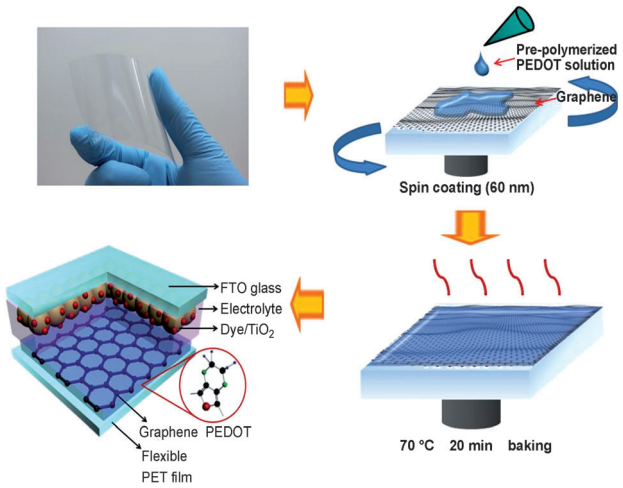

Figure 1. Photograph of a graphene-coated PET substrate, and schematic diagram of the fabrication steps involved in preparing a DSSC with a graphene/PEDOT counter electrode on a PET substrate.

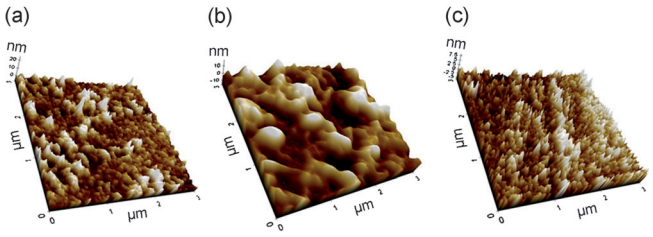

Figure 2. AFM images of (a) bare PET substrate, (b) typical rippled structures of graphene layers, and (c) a graphene electrode covered with PEDOT film.

sorbed onto the copper surface at 1000 °C, two-dimensional atomic structures are formed during a cooling process in an atmosphere of hydrogen. In the transfer process, PMMA is coated onto the graphene film on the copper foil used as a supporting layer during the transfer process. The minor graphene layer on the back-side of the copper foil is removed by an oxygen plasma process to expose the copper to its etchant. The copper foil is removed by ammonium persulfate solution (ca. 0.1 M). Finally, the PMMA/graphene layers are transferred onto the PET substrate in water. Repeating this process results in a randomly stacked graphene film structure. Raman spectra of graphene film revealed an I_{2D}/I_G ratio of ca. 2.5 and a negligible intensity of the D-band. In addition, the transmittance values of the mono- and four-layered graphene films were ca. 97.4% and ca. 90.6%, respectively, at $\lambda = 550$ nm. These properties indicate that monolayer graphene film with low amount of defects is dominantly synthesized on copper by CVD method (Figure S1).[24]

To enhance the conductance of the graphene films, they were chemically doped by using nitric acid. A nitric acid treatment of a few seconds can reduce their sheet resistance to as much as ca. 60 $\Omega\,sq^{-1}$ (Figure S2). Then, a PEDOT thin film (ca. 110 nm) was fabricated on the graphene layers by a modified simple presolution/in situ polymerization method, as reported elsewhere.[17]

The sheet resistances of the PEDOT film, graphene film, and graphene/PEDOT composite film were 141 $\Omega\,sq^{-1}$, 60 $\Omega\,sq^{-1}$, and 62 $\Omega\,sq^{-1}$, respectively. Images taken by atomic force microscopy (AFM) image shows the typical rippled structures of graphene layers (Figure 2b). The root-mean-square (RMS) roughness values of the bare PET, graphene-coated PET, and the graphene/PEDOT film were 2.7 nm, 5.2 nm, and 2.2 nm, respectively. A very smooth surface morphology was observed after covering the graphene electrode with the PEDOT film (Figure 2c). To investigate the oxidation/reduction ability of the electrolyte in the DSSC, the cyclic voltammograms of the various electrodes in an I^-/I_3^- redox solution were measured. The results are shown in Figure 3a. All of the electrodes exhibited oxidation/reduction shapes similar to those of a Pt/ITO counter electrode. The oxidation/reduction peak current densities of the graphene/PEDOT counter electrode were slightly larger than those of the pure PEDOT electrodes. These results imply that the incorporation of graphene into PEDOT results in not only superior electrochemical activity, but also much faster charge transport through the composite film. However, the reduction potential to yield from triiodide to iodide in the graphene/PEDOT counter electrode was shifted negatively compared to that of a Pt/ITO electrode (the peak between −0.6 V and 0 V), which means that the platinum- and TCO-free counter electrode still has a larger resistance.

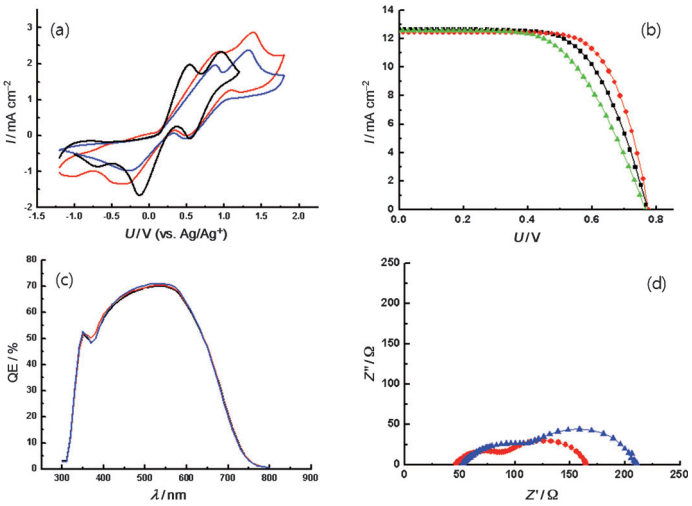

Figure 3. (a) Cyclic voltammograms of DSSCs using as counter electrode: —— graphene/PEDOT/PET, ——PEDOT/PET, and —— Pt/ITO/PEN, cycled in I^-/I_3^- electrolyte (10 mM LiI+1 mM I_2+0.1 M $LiClO_4$+acetonitrile) at a scan rate of 100 mV s^{-1}. (b) *J–V* characteristics of DSSCs using as counter electrode ■ graphene/PEDOT/PET, ▲ PEDOT/PET, and ● Pt/ITO/PEN. (c) IPCE spectra of the DSSCs using as counter electrode: —— graphene/PEDOT/PET, ——PEDOT/PET, and —— Pt/ITO/PEN. (d) Nyquist plots of DSSCs using as counter electrode: ▲ PEDOT/PET ● graphene/PEDOT/PET.

The cell performances with the different counter electrodes were compared directly with that of a Pt/ITO counterpart by using the same TiO_2 layer thickness, dye, electrolyte, and cell

assembly method. Figure 3b shows the photocurrent (J) and photovoltage (V) of the DSSC measured with an active area of ca. 0.15 cm^2 using simulated solar light at AM 1.5 produced by a 150 W xenon lamp (Oriel, 91193). The addition of the graphene layers between the conducting polymer and substrate was beneficial for the enhancement of the fill factor (FF), while maintaining the other parameters. The thickness of the TiO_2 layer was controlled to be ca. 10 μm without an additional light scattering layer. The J–V characteristics of the devices with the platinum-coated ITO substrate and the PEDOT-only counter electrodes are also shown in Figure 3b. The Pt/ITO counter electrode-based DSSC exhibited a J_{sc} of 12.4 mA cm^{-2}, a V_{oc} of 0.77 V, an FF of 0.70, and an overall conversion efficiency of 6.68%. The DSSC based on the pure PEDOT counter electrode showed a J_{sc} of 12.6 mA cm^{-2}, a V_{oc} of 0.77 V, an FF of 0.58, and an overall conversion efficiency of 5.62%. However, the main problem of the PEDOT-based platinum- and FTO-free (FTO = fluorine-doped tin oxide) counter electrodes are their poor FF values. The FF of the DSSC with a graphene/PEDOT counter electrode was greatly improved to 0.63 while maintaining the other parameters, such as the J_{sc} and V_{oc}, resulting in an overall conversion efficiency of 6.26%. As shown in Figure 3c, the incident photon conversion efficiency (IPCE) spectrum of the DSSCs with graphene/PEDOT is comparable to that of the Pt/ITO-based DSSC. Finally, as the composite film shows a good transmittance of more than 70% (at $\lambda =$ 500 nm), the transparency of the graphene/PEDOT-based DSSC is similar to DSSCs with platinum-based counter electrodes (Supporting Information, Figure S3).

When PEDOT was coated onto a TCO substrate and used as the counter electrode, a much higher cell efficiency was obtained than when using a PEDOT-only counter electrode (Figure S4). The lower efficiency of the pure-PEDOT DSSC is due to the higher sheet resistance. Therefore, the enhanced FF following the incorporation of graphene layers originates from the decreased surface resistance. Figure S5 shows a J–V curve of a DSSC with a platinum- and TCO-free counter electrode composed of only graphene layers on a PET substrate. Pure graphene does not function well as a counter electrode in the DSSC. When multilayered graphene is in direct contact with the electrolyte, delamination of the stacked graphenes is observed. This result shows that the pure graphene layers are not stable in the organic electrolyte. The overcoated PEDOT layer can prevent direct contact between the electrolyte and the graphene sheets.

To understand the effect of inserting graphene, an impedance analysis was done. The Nyquist plot is shown in Figure 3d. In all of the EIS Cole–Cole plots, two well-defined semicircles can be observed, in the high- (>1 kHz) and medium-frequency (1 ~ 100 Hz) regions. In the high-frequency region, different bulk resistances of the DSSC were observed, corresponding to electron transport processes in the solid state with very short time constants. The graphene layers in the counter electrode decrease in the bulk resistance, from 59 Ω to 41 Ω. The high-frequency semicircle corresponds to the I^-/I_3^- redox reaction at the counter electrodes. The decreased size of the first semicircle is attributed to the positive effect of inserting graphene between the substrate and PEDOT. Mechanical flexibility and robustness are important characteristics of flexible DSSCs. Before assembling the photoanode and counter electrode, a symmetric bending test was performed on the different counter electrodes (bending radius: 0.47, bending number: 10). We then compared the J–V curves of the DSSCs before and after the bending test. Figure 4 shows

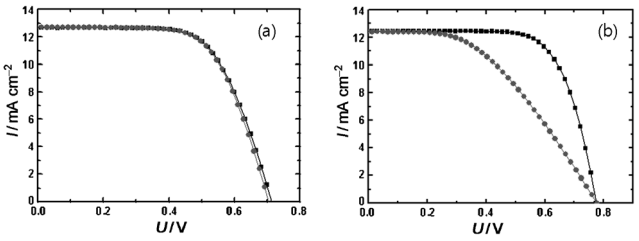

Figure 4. J–V characteristics of ● bent and ■ pristine DSSCs using (a) graphene/PEDOT as counter electrode, and (b) ITO/PEDOT as counter electrode.

the changes in cell performance. In DSSCs with a PEDOT/ITO counter electrode, the cell performance is strongly degraded after the bending test, because the ITO cannot support the tension. However, the graphene/PEDOT counter electrode shows almost the same cell performance after the bending test.

In conclusion, we demonstrate the effect of inserting graphene between PEDOT and the substrate in TCO- and platinum-free counter electrodes in DSSCs. The highly conductive PEDOT film takes over the role of both platinum and TCO. Moreover, the graphene sheet enhances electron transport and so decreases the surface resistance. The graphene/PEDOT films without TCO and platinum are used as counter electrode in DSSCs, resulting in a power conversion efficiency of 6.26%, while the efficiencies of DSSCs with Pt/ITO and PEDOT counter electrodes are 6.68% and 5.62%, respectively. To eliminate the need for platinum and TCO in the counter electrodes of large-area DSSCs, new materials with improved electrical conductivity and electrocatalytic properties matching, or possibly exceeding, those of platinum need to be introduced. We believe that the graphene/PEDOT composite film is a good candidate material.

Experimental Section

Graphene synthesis: First, the copper foils were inserted into a tubular quartz tube and heated to 1000 °C at low pressure (ca. 11.6 Pa) at a H_2 flow rate of 10 sccm. At 1000 °C, H_2 treatment under the same conditions was maintained for 30 min. After flowing the reaction gas mixtures $CH_4/H_2 = 15{:}10$ sccm) for 30 min, the sample was rapidly cooled down to room temperature.

Preparation of graphene/PEDOT composite film on PET: The PEDOT thin film was synthesized on the graphene-coated PET substrate by a modified pre-solution/in situ polymerization method. First, the monomer solution was prepared by dissolving 3,4-ethylenedioxythiophene (EDOT), poly(vinyl pyrrolidone) as a matrix polymer, and pyridine as a retardant in 1-butanol or etha-

nol. An oxidant solution was separately prepared by dissolving ferric *p*-toluene sulfonate (FTS) in 1-butanol or ethanol. The EDOT-based and FTS-based solutions were then mixed. Then, prepolymerization was conducted at temperatures ranging from 5 to 30 °C for 3 to 72 h. The prepolymerized PEDOT solution was coated onto the graphene-covered substrate to form a prepolymerized PEDOT film. The graphene/PEDOT film was obtained by post-polymerization at 70 °C for 20 min, followed by washing with methanol and drying, resulting in the final film.

Fabrication of DSSCs: FTO glass was rinsed successively with acetone, ethanol, and deionized water for 10 min each and then dried in nitrogen. Then, an underlayer was coated on FTO using 20 mM $TiCl_4$ (Aldrich) at 70 °C for 30 min and rinsed with ethanol. Commercialized TiO_2 paste (Dyesol) was coated on the underlayer by the doctor-blading method. The resulting TiO_2 films were calcined at 550 °C for 30 min and then slowly cooled to room temperature. Subsequently, the sintered TiO_2 films were immersed in ethanol containing 0.3 mM N719 dye for 18 h. For the reference DSSC, the counter electrode was prepared by coating 40 mM hydrogen hexachloroplatinate (IV) hydrate in 2-propanol on ITO/PET substrate. Then, a 60 mM reducing agent was prepared by dissolving $NaBH_4$ in an H_2O/ethanol mixture (8:2 vol. ratio). Pt^{IV}-coated plastics were immersed in the reducing agent solution until the surface became dark. The treated samples were washed by ethanol and water sequentially, and were dried for 2 h at 130 °C. The dye-adsorbed TiO_2 film and platinum-coated or graphene/PEDOT counter electrode were sealed using Hot Melt surlyn (50 μm thickness), and then the electrolyte was injected into the hole of the counter electrode by capillary action.

Characterization: Four-point probe measurements taken to measure surface resistance. The photovoltaic properties of the solar cells were measured by using a Keithley model 2400 source measuring unit under 100 mW cm^{-2} illumination using a 1000 W xenon lamp (Spectra-Physics) as light source. The IPCE was measured as a function of the wavelength from 400 nm to 800 nm using a specially designed IPCE system for dye-sensitized solar cells (PV Measurement, Inc.). The electrochemical impedance spectra and cyclic voltammograms were measured under 100 mW cm^{-2} illumination at open-circuit voltage by a potentiostat (CH Instruments, CHI 608C). For surface roughness measurements, atomic force microscopy (AFM, SPA-300HV) was used.

Acknowledgements

This research was supported by an NRF grant funded by the Korean government (MEST) (2009–0092950, 2011–0030254), the NCRC program (2011–0006268), and the Future-based Technology Development Program (2010–0029321).

Keywords: dyes · electrochemistry · graphene · platinum · solar cells

[1] P. S. Wang, M. Zakeeruddin, P. Comte, I. Exnar, M. Grätzel, *J. Am. Chem. Soc.* **2003**, *125*, 1166 – 1167.
[2] B. O'Regan, M. Grätzel, *Nature* **1991**, *353*, 737 – 740.
[3] A. Hagfeldt, M. Grätzel, *Acc. Chem. Res.* **2000**, *33*, 269 – 277.
[4] J. H. Park, Y. S. Jun, H. K. Yoon, S. Y. Lee, M. G. Kang, *J. Electrochem. Soc.* **2008**, *155*, F145 – F149.
[5] G. Smestad, C. Bignozzi, R. Argazzi, *Sol. Energy Mater. Sol. Cells* **1994**, *32*, 259 – 272.
[6] J.-C. Tinguely, R. Solarska, A. Braun, T. Graule, *Semicond. Sci. Technol.* **2011**, *26*, 045007.
[7] C. Y. Jiang, X. W. Sun, K. W. Tan, G. Q. Lo, A. K. K. Kyaw, D. L. Kwong, *Appl. Phys. Lett.* **2008**, *92*, 143101.
[8] W. Hong, Y. Xu, G. Lu, C. Li, G. Shi, *Electrochem. Commun.* **2008**, *10*, 1555 – 1558.
[9] N. Papageorgiou, P. Liska, A. Kay, M. Grätzel, *J. Electrochem. Soc.* **1999**, *146*, 898 – 907.
[10] N. Papageorgiou, W. F. Maier, M. Grätzel, *J. Electrochem. Soc.* **1997**, *144*, 876 – 884.
[11] K. Suzuki, M. Yamaguchi, M. Kumagai, S. Yanagida, *Chem. Lett.* **2003**, *32*, 28 – 29.
[12] K. Imoto, K. Takahashi, T. Yamaguchi, T. Komura, J. Nakamura, K. Murata, *Sol. Energy Mater. Sol. Cells* **2003**, *79*, 459 – 469.
[13] a) T. N. Murakami, S. Ito, Q. Wang, M. K. Nazeeruddin, T. Bessho, I. Cesar, P. Liska, R. Humphry-Baker, P. Comte, P. Pechy, M. Grätzel, *J. Electrochem. Soc.* **2006**, *153*, A2255A2261. b) H. Choi, H. Kim, S. Hwang, Y. Han, M. Jeon, *J. Mater. Chem.* **2011**, *21*, 7548 – 7551.
[14] K. M. Lee, P. Y. Chen, C. Y. Hsu, H. H. Huang, W. H. Ho, H. C. Chen, K. C. Ho, *J. Power Sources* **2009**, *188*, 313 – 318.
[15] a) Q. Li, J. Wu, Q. Tang, Z. Lan, P. Li, J. Lin, L. Fan, *Electrochem. Commun.* **2008**, *10*, 1299 – 1302; b) K. C. Huang, J. H. Huang, C. H. Wu, C. Y. Liu, H. W. Chen, C. W. Chu, J. Lin, C. L. Lin, K. C. Ho, *J. Mater. Chem.* **2011**, *21*, 10384 – 10389.
[16] S. Ahmad, J. H. Yum, Z. Xianxi, M. Grätzel, H. J. Butt, M. K. Nazeeruddin, *J. Mater. Chem.* **2010**, *20*, 1654 – 1658.
[17] K. S. Lee, H. K. Lee, D. H. Wang, N. G. Park, J. Y. Lee, O. O. Park, J. H. Park, *Chem. Commun.* **2010**, *46*, 4505 – 4507.
[18] a) S. Pang, Y. Hernandez, X. Feng, K. Müllen, *Adv. Mater.* **2011**, *23*, 2779 – 2795; b) A. K. Geim, *Science* **2009**, *324*, 1530 – 1534.
[19] K. S. Novoselov, A. K. Geim, S. V. Morozov, D. Jiang, M. I. Katsnelson, I. V. Grigorieva, S. V. Dubonos, A. A. Firsov, *Nature* **2005**, *438*, 197 – 200.
[20] Y. Zhang, J. W. Tan, H. L. Stormer, P. Kim, *Nature* **2005**, *438*, 201 – 204.
[21] J. A. Rogers, *Nat. Nanotechnol.* **2008**, *3*, 254 – 255.
[22] B. J. Kim, H. Jang, S. K. Lee, B. H. Hong, J. H. Ahn, J. H. Cho, *Nano Lett.* **2010**, *10*, 3464 – 3466.
[23] Y. Lee, S. Bae, H. Jang, S. Jang, S.-E. Zhu, S. H. Sim, Y. I. Song, B. H. Hong, J. H. Ahn, *Nano Lett.* **2010**, *10*, 490 – 493.
[24] S. Bae, H. Kim, Y. Lee, X. Xu, J. Park, Y. Zheng, J. Balakrishnan, D. Im, T. Lei, H. R. Kim, Y. Song, Y. Kim, K. Kim, B. Ozyimaz, J. Ahn, B. Hong, S. Iijima, *Nat. Nanotechnol.* **2010**, *5*, 574 – 578.

Received: August 5, 2011
Revised: September 2, 2011
Published online on January 13, 2012

